

# Vacuum polarization of massive scalar fields in the spacetime of the electrically charged nonlinear black hole

Jerzy Matyjasek\*

*Institute of Physics, Maria Curie-Skłodowska University,  
pl. Marii Curie - Skłodowskiej 1,  
20-031 Lublin, Poland*

The approximate renormalized stress-energy tensor of the quantized massive conformally coupled scalar field in the spacetime of electrically charged nonlinear black hole is constructed. It is achieved by functional differentiation of the lowest order of the DeWitt-Schwinger effective action involving coincidence limit of the Hadamard-Minakshisundaram-DeWitt-Seely coefficient  $a_3$ . The result is compared with the analogous results derived for the Reissner-Nordström black hole. It is shown that the most important differences occur in the vicinity of the event horizon of the black hole near the extremality limit. The structure of the nonlinear black hole is briefly studied by means of the Lambert functions.

PACS numbers: 04.70.Dy, 04.62+v  
UMCS-TG-00-18

## I. INTRODUCTION

For the quantized massive fields in the large mass limit, i. e., when the Compton length is much smaller than the characteristic radius of a curvature, the nonlocal contribution to the effective action can be neglected, and the series expansion in  $m^{-2}$  of the renormalized effective action,  $W_R$ , may be easily constructed with the aid of the DeWitt-Schwinger method [1,2]. As the renormalization prescription requires absorption of the first three terms of the series into the quadratic classical gravitational action, the  $n$ -th term of  $W_R$  is proportional to the integrated coincidence limit of the Hadamard-Minakshisundaram-DeWitt-Seely coefficient (HMDS)  $a_{n+3}$ . Unfortunately, the complexity of the coefficients  $[a_n]$  rapidly increases with  $n$ , and consequently one expects that the applicability of the series expansion is confined to a first, perhaps a second nonvanishing term.

Having constructed a first order  $W_R$ , the renormalized stress-energy tensor (which is the most important characteristics of the quantized field in the curved spacetime) may be obtained in a standard way, i. e., by functional differentiating the constructed effective action with respect to the metric tensor. This method has been successfully applied in calculations of the approximate renormalized stress-energy tensor of the quantized massive scalar, spinor, and vector fields in the vacuum type-D geometries by Frolov and Zel'nikov [3-7].

A different method, based on the WKB approximation of the solutions of the massive scalar field equation in a general spherically-symmetric spacetime, and summation thus ob-

---

\*Electronic Address: matyjase@tytan.umcs.lublin.pl, jurek@iris.umcs.lublin.pl

tained modes by means of the Abel-Plana formula, has been invented by Anderson, Hiscock, and Samuel and applied in the context of the RN spacetime [8]. Their method is equivalent to the Schwinger - DeWitt expansion: to obtain the lowest (i. e.  $m^{-2}$ ) terms, one has to use sixth-order WKB approximation. Moreover, numerical calculations reported in Ref.[8] confirmed that the DeWitt-Schwinger method provide a good approximation of the renormalized stress-energy tensor of the massive scalar field with arbitrary curvature coupling as long as the mass of the field remains sufficiently large. This approach and its modifications has been employed in various contexts in Refs.[9-15].

Recently, extending the results of Frolov-Zel'nikov, we have constructed a general formula describing the approximate renormalized  $\langle T_a^b \rangle_{ren}$  of the quantized massive scalar, spinor, and vector fields in arbitrary spacetime. The results have been presented for the class of geometries with vanishing curvature scalar, and subsequently applied in the spacetime of the RN black hole and in the spacetime that could be obtained by expanding its near horizon geometry into a whole manifold [16]. Our formulas allow, in principle, to determine the renormalized stress-energy tensor of the massive field once the line element has been chosen, although the specific calculations may be very tedious. For the quantized massive scalar field with arbitrary curvature coupling in the RN spacetime we have reproduced the results of Anderson, Hiscock, and Samuel; neutral spinor and vector fields have not been discussed earlier.

In this paper we shall extend the analyses of Ref.[16] to the general geometry and construct the renormalized stress-energy tensor of the massive quantized scalar field obeying the equation

$$\left(-\square + \xi R + m^2\right) \phi = 0, \tag{1}$$

where  $\xi$  is the coupling constant and  $m$  is the mass of the field. Since the background geometry is general, the most direct approach is to use the first nonvanishing term of the renormalized effective action. The advantage of this approach lies in the purely geometric nature of the approximation that reflects its local nature. Although the constructed result is rather complex, we shall present it in its full length, because it provides the generic formula from which the renormalized stress-energy tensor in some physically interesting cases may be easily obtained. As the effective action of the quantized massive scalar field differs from the analogous actions constructed for fields of higher spins only by numerical coefficients, one can generalize presented results to fields of other spins. It should be emphasized however, that the method has obvious limitations, and, when applied to rapidly varying or strong gravitational fields it breaks down. Moreover, its massless limit is contaminated by nonphysical divergences.

Our general formulas will be employed in the calculations of  $\langle T_a^b \rangle_{ren}$  in the geometry of the electrically charged black hole, being an exact solution of the coupled system of the Einstein equations and the equations of the nonlinear electrodynamics recently proposed by Ayón-Beato and García (ABG) in Ref. [17], to which the reader is referred for physical motivations and technical details. Their exact solution is characterized by the electric charge,  $e$  and the mass  $M$ , and may be elegantly expressed in terms of the hyperbolic functions. An important and interesting feature of this solution is its regularity as radial coordinate tends to zero. We shall show that the structure of horizons of the ABG solution may be studied by means of the Lambert function [18], allowing analytical treatment of the vacuum

polarization effects on the event horizon. At large distances their solution behaves as the RN solution. For small and intermediate values of the ratio  $|e|/M$ , the location of the event horizon,  $r_+$ , is close to the location of the event horizon of the RN black hole; significant differences occur near the extremality limit. It would be, therefore, interesting to analyze how the similarities of the line elements are reflected in the behavior of the renormalized stress-energy tensors.

The renormalized effective action of the massive scalar field involves the terms that are proportional to the first and third power of  $\xi - 1/6$ . As the curvature scalar of the RN spacetime vanishes,  $\langle T_a^b \rangle_{ren}$  of the massive scalar field naturally divides into the part that describes pure conformal coupling and an additional local part that is multiplied by a factor  $\xi - 1/6$ . On the other hand however, the curvature scalar of the ABG geometry does not vanish, and the structure of the effective action indicates that the renormalized stress-energy tensor of the massive scalar depends on the constant  $\xi$  in a more complicated way. Since the conformal coupling leads to massive simplifications, one expects that the similarities in the renormalized  $\langle T_a^b \rangle_{ren}$  (if any) would appear mainly in this case.

## II. THE RENORMALIZED STRESS-ENERGY TENSOR OF THE QUANTIZED MASSIVE SCALAR FIELD

The renormalized effective action constructed for the quantized scalar field satisfying equation (1) is given by

$$W_{ren} = \frac{1}{32\pi^2 m^2} \int d^4x g^{1/2} \sum_{n=3}^{\infty} \frac{(n-3)!}{(m^2)^{n-2}} [a_n], \quad (2)$$

where  $[a_n]$  is the coincidence limit of the  $n$ -th HDSM coefficient. The first three coefficients of the DeWitt-Schwinger expansion,  $a_0$ ,  $a_1$ , and  $a_2$ , which contribute to the divergent part of the action have to be absorbed in the classical gravitational action by renormalization of the bare coupling constant.

As the rigorous asymptotic analysis of the fundamental solution is restricted, in general, to the heat operator of a parabolic type, we tacitly assume that all steps that are necessary in construction of the first-order renormalized stress-energy tensor have been carried out in an analytically continued Euclidean spacetime. The analytic continuation to the physical space is performed at the last stage of the calculations.

Calculation of the HDSM coefficients is an extremely laborious task, and their exact form for  $n \geq 5$  is unknown. The coefficient  $[a_2]$ , which is proportional to the trace anomaly of the renormalized stress-energy tensor of the quantized, massless, and conformally invariant fields, has been calculated by DeWitt [1]. The coincidence limit of the coefficient  $a_3$  has been obtained by Gilkey [19,20] whereas the coefficient  $[a_4]$  has been calculated by Avramidi [21-24].

Restricting ourselves to the terms proportional to  $m^{-2}$ , one has

$$W_{ren} = \frac{1}{32\pi^2 m^2} \int d^4x g^{1/2} [a_3], \quad (3)$$

with

$$[a_3] = \frac{b_3}{7!} + \frac{c_3}{360}, \quad (4)$$

where

$$\begin{aligned} b_3 = & \frac{35}{9}R^3 + 17R_{;p}R^{;p} - R_{qa;p}R^{qa;q} - 4R_{qa;p}R^{pa;q} \\ & + 9R_{qabc;p}R^{qabc;p} + 2R\Box R + 18\Box^2 R - 8R_{pq}\Box R^{pq} - \frac{14}{3}RR_{pq}R^{pq} \\ & + 24R_{pq;a}R^{pa} - \frac{208}{9}R_{pq}R^{qa}R_a{}^p + 12\Box R_{pqab}R^{pqab} + \frac{64}{3}R_{pq}R_{ab}R^{pqab} \\ & - \frac{16}{3}R_{pq}R^{pabc}R^{qabc} + \frac{80}{9}R_{pqab}R_c{}^p{}^a R^{qcbd} + \frac{44}{9}R_{pqab}R_{cd}{}^{pq}R^{abcd} \end{aligned} \quad (5)$$

and

$$\begin{aligned} c_3 = & -(5\xi - 30\xi^2 + 60\xi^3)R^3 - (12\xi - 30\xi^2)R_{;p}R^{;p} - (22\xi - 60\xi^2)R\Box R \\ & - 6\xi\Box^2 R - 4\xi R_{pq}R^{pq} + 2\xi RR_{pq}R^{pq} - 2\xi RR_{pqab}R^{pqab}. \end{aligned} \quad (6)$$

Since the coincidence limit of the coefficient  $a_4$  is much more complex one expects that using it in the calculations of the approximate renormalized stress-energy would be a real challenge. However, it still could be of use in the simpler analyses of the field fluctuation,  $\langle\phi^2\rangle_{ren}$ . Substituting (4-6) into (3), integrating by parts and making use of elementary properties of the Riemann tensor, one can reduce the number of terms in the renormalized effective action to ten [21]:

$$\begin{aligned} W_{ren}^{(1)} = & \frac{1}{192\pi^2 m^2} \int d^4x g^{1/2} \left[ \left( \frac{1}{2}\xi^2 - \frac{1}{5}\xi + \frac{1}{56} \right) R\Box R + \frac{1}{140} R_{pq}\Box R^{pq} \right. \\ & + \left( \frac{1}{6} - \xi \right)^3 R^3 - \frac{1}{30} \left( \frac{1}{6} - \xi \right) RR_{pq}R^{pq} + \frac{1}{30} \left( \frac{1}{6} - \xi \right) RR_{pqab}R^{pqab} \\ & - \frac{8}{945} R_q{}^p R_a{}^q R_p{}^a + \frac{2}{315} R^{pq} R_{ab} R_p{}^a{}^b{}^q + \frac{1}{1260} R_{pq} R^p{}_{cab} R^{qcab} \\ & \left. + \frac{17}{7560} R_{ab}{}^{pq} R_{pq}{}^{cd} R_{cd}{}^{ab} - \frac{1}{270} R_p{}^a{}^b{}^q R_c{}^p{}^q{}^d R^c{}^d{}_{ab} \right] \\ = & \frac{1}{192\pi^2 m^2} \sum_{i=1}^{10} \alpha_i W_i, \end{aligned} \quad (7)$$

where  $\alpha_i$  are numerical coefficients that stand in front of the geometrical terms.

The renormalized stress-energy tensor is given by the standard relation

$$\frac{2}{g^{1/2}} \frac{\delta}{\delta g_{ab}} W_{ren}^{(1)} = \langle T^{ab} \rangle_{ren}. \quad (8)$$

Functionally differentiating the renormalized effective action with respect to the metric tensor, performing simplifications and necessary symmetrizations, after rather long calculations, one has

$$\begin{aligned} \frac{1}{g^{1/2}} \frac{\delta}{\delta g_{mn}} W_1 = & R^{;m} R^{;n} + (\Box R)^{;mn} + (\Box R)^{;nm} \\ & - \frac{1}{2} R_{;p} R^{;p} g^{mn} - 2\Box^2 R g^{mn} - 2\Box R R^{mn}, \end{aligned} \quad (9)$$

$$\begin{aligned}
\frac{1}{g^{1/2}} \frac{\delta}{\delta g_{mn}} W_2 &= R_{pq}{}^{;m} R^{pq;n} - R_{pq}{}^{;n} R^{pm;q} - R_{pq}{}^{;m} R^{pn;q} \\
&\quad + R_{pq}{}^{;p} R^{qm;n} + R_{pq}{}^{;p} R^{qn;m} + (\square R_p{}^m)^{;np} \\
&\quad + (\square R_p{}^n)^{;mp} - \square^2 R^{mn} - \frac{1}{2} R_{pq;r} R^{pq;r} g^{mn} \\
&\quad - (\square R_{pq})^{;qp} g^{mn} + R_p{}^{m;n} R^{pq} + R_p{}^{n;m} R^{pq} \\
&\quad - R_{pq}{}^{;nq} R^{pm} - \square R_p{}^n R^{pm} - \square R_p{}^m R^{pn} \\
&\quad - R_{pq}{}^{;mq} R^{pn}, \tag{10}
\end{aligned}$$

$$\begin{aligned}
\frac{1}{g^{1/2}} \frac{\delta}{\delta g_{mn}} W_3 &= 6R^{;m} R^{;n} + 6RR^{mn} + \frac{1}{2} R^3 g^{mn} \\
&\quad - 6R_{;p} R^{;p} g^{mn} - 6R \square R g^{mn} - 3R^2 R^{mn}, \tag{11}
\end{aligned}$$

$$\begin{aligned}
\frac{1}{g^{1/2}} \frac{\delta}{\delta g_{mn}} W_4 &= R^{;n} R_p{}^{m;p} + R^{;m} R_p{}^{n;p} + 2R_{pq}{}^{;n} R^{pq;m} \\
&\quad + R_{;p} R^{pm;n} + R_{;p} R^{pn;m} - 2R_{;p} R^{mn;p} \\
&\quad + RR_p{}^{m;n} + RR_p{}^{n;m} - R \square R^{mn} \\
&\quad - 2R_{;p} R_q{}^{p;q} g^{mn} - 2R_{pq;r} R^{pq;r} g^{mn} - RR_{pq}{}^{;qp} g^{mn} \\
&\quad + R_{pq}{}^{;mn} R^{pq} + R_{pq}{}^{;nm} R^{pq} + R_{;pq} R^{pq} g^{mn} \\
&\quad - 2 \square R_{pq} R^{pq} g^{mn} + \frac{1}{2} RR_{pq} R^{pq} g^{mn} + R_{;p}{}^n R^{pm} \\
&\quad - 2RR_p{}^n R^{pm} + R_{;p}{}^m R^{pn} - \square RR^{mn} \\
&\quad - R_{pq} R^{pq} R^{mn}, \tag{12}
\end{aligned}$$

$$\begin{aligned}
\frac{1}{g^{1/2}} \frac{\delta}{\delta g_{mn}} W_5 &= -4R_{;p} R_q{}^{mpn;q} - 4R_{;p} R_q{}^{npm;q} + 2R_{pqrs}{}^{;n} R^{pqrs;m} \\
&\quad - 2RR_{pq}{}^{m;n} R^{qp} - 2RR_{pq}{}^{n;m} R^{qp} - 2R_{pqrs;t} R^{pqrs;t} g^{mn} \\
&\quad + R_{pqrs}{}^{;mn} R^{pqrs} + R_{pqrs}{}^{;nm} R^{pqrs} - 2 \square R_{pqrs} R^{pqrs} g^{mn} \\
&\quad + \frac{1}{2} RR_{pqrs} R^{pqrs} g^{mn} - R^{mn} R_{pqrs} R^{pqrs} - 2RR_{pqr}{}^n R^{pqrm} \\
&\quad - 2R_{;pq} R^{pmqn} - 2R_{;pq} R^{pnqm}, \tag{13}
\end{aligned}$$

$$\begin{aligned}
\frac{1}{g^{1/2}} \frac{\delta}{\delta g_{mn}} W_6 &= \frac{3}{2} R_{pq}{}^{;n} R^{pm;q} + \frac{3}{2} R_{pq}{}^{;m} R^{pn;q} - 3R_p{}^m R^{pn;q} \\
&\quad + \frac{3}{2} R_{pq}{}^{;p} R^{qm;n} + \frac{3}{2} R_{pq}{}^{;p} R^{qn;m} - \frac{3}{2} R_{pq}{}^{;p} R_r{}^{q;r} g^{mn} \\
&\quad - \frac{3}{2} R_{pq;r} R^{pr;q} g^{mn} + \frac{3}{2} R_p{}^{m;n} R^{pq} + \frac{3}{2} R_p{}^{n;m} R^{pq} \\
&\quad - \frac{3}{2} R_{pq;r}{}^q R^{pr} g^{mn} + \frac{3}{2} R_{pq}{}^{;nq} R^{pm} - \frac{3}{2} \square R_p{}^n R^{pm} \\
&\quad + \frac{3}{2} R_{pq}{}^{;mq} R^{pn} - \frac{3}{2} \square R_p{}^m R^{pn} - \frac{3}{2} R_{pq}{}^{;p} R_r{}^{qr} g^{mn} \\
&\quad + R_{pq} R_r{}^p R^{qr} - 3R_{pq} R^{pm} R^{qn}, \tag{14}
\end{aligned}$$

$$\begin{aligned}
\frac{1}{g^{1/2}} \frac{\delta}{\delta g_{mn}} W_7 &= R_p^{m;p} R_q^{n;q} + R_p^n R^{qm;p} - 2R_{pq}{}^p R^{mn;q} \\
&\quad - R_{pq}{}^n R_r{}^{pqm;r} - R_{pq}{}^m R_r{}^{pqn;r} + R_{pq;r} R^{prqm;n} \\
&\quad + R_{pq;r} R^{prqn;m} - 2R_{pq;r} R^{pmqn;r} + 2R_{pq;r} R_s{}^{pqr;s} g^{mn} \\
&\quad - R^{mn}{}_{;pq} R^{pq} + R_p^m{}_{;qr} R^{pq} - \square R_p^m{}_{;q} R^{pq} \\
&\quad + R_p^n{}_{;qr} R^{pq} - R_{pqr;s}{}^{sq} R^{pr} g^{mn} + \frac{1}{2} R_p^n{}_{;q} R^{qm} \\
&\quad + \frac{1}{2} R_p^n{}_{;p} R^{qm} + \frac{1}{2} R_p^m{}_{;q} R^{qn} + \frac{1}{2} R_p^m{}_{;q} R^{qn} \\
&\quad - R_{pq}{}^{qp} R^{mn} + \frac{1}{2} R_{pq} R_{rs} R^{prqs} + R_{pq}{}^n R_r{}^{prqm} \\
&\quad - \frac{3}{2} R_{pq} R_r{}^n R^{prqm} + R_{pq}{}^m R_r{}^{prqn} - \frac{3}{2} R_{pq} R_r{}^m R^{prqn} \\
&\quad - R_{pq;rs} R^{psqr} g^{mn} - \square R_{pq} R^{pmqn}, \tag{15}
\end{aligned}$$

$$\begin{aligned}
\frac{1}{g^{1/2}} \frac{\delta}{\delta g_{mn}} W_8 &= -2R_p^m{}_{;q} R_r{}^{pqn;r} + 2R_p^m{}_{;q} R_r{}^{npq;r} - 2R_{pq}{}^p R_r{}^{nqm;r} \\
&\quad + R_{pqr;s}{}^n R^{pqrm;s} - R_{pqr;s}{}^m R^{pqrn;s} - 2R_{pq;r} R^{pmrn;q} \\
&\quad - R_{pqr;s}{}^p R^{qmrs;n} - \frac{1}{2} R_{pqr;s}{}^p R_t{}^{qrs;t} g^{mn} - \frac{1}{2} R_{pqr;s;t} R^{pqrt;s} g^{mn} \\
&\quad - 2R_p^n{}_{;q} R_r{}^{pqr} - 2R_{pqr}{}^{n;rp} R^{qm} + 2R_p^m{}_{;qr} R^{prqn} \\
&\quad + R_p^m{}_{;qr}{}^n R^{psqr} + R_p^m R_{qrs}{}^n R^{psqr} - \frac{1}{2} R_{pqr;s;t}{}^q R^{ptrs} g^{mn} \\
&\quad - \frac{1}{2} \square R_p^n{}_{;qr} R^{pmqr} + R_{pqr;s}{}^{nq} R^{pmrs} - \frac{1}{2} \square R_p^m{}_{;qr} R^{pnqr} \\
&\quad + 2R_{pq} R_r{}^p{}^m R^{qrsn} + \frac{1}{2} R_{pqr;s}{}^p R_t{}^{qtrs} g^{mn} - \frac{1}{2} R_{pq} R_{rst}{}^p R^{qtrs} g^{mn} \\
&\quad - 2R_{pq;r}{}^p R^{qmrn}, \tag{16}
\end{aligned}$$

$$\begin{aligned}
\frac{1}{g^{1/2}} \frac{\delta}{\delta g_{mn}} W_9 &= -6R_{pqr}{}^{n;r} R_s{}^{mpq;s} - 6R_{pqr}{}^n R^{pqsm;r} - 3R_{pqr}{}^m R_{st}{}^{rn} R^{pqst} \\
&\quad - 3R_{pqr}{}^n{}^r R^{pqsm} - 3R_{pqr}{}^m{}^r R^{pqsn} - 3R_p^n{}_{;qr}{}^p R^{qrsn} \\
&\quad - 3R_p^m{}_{;qr}{}^p R^{qrsn} + \frac{1}{2} R_{pqr;s} R_{tu}{}^{pq} R^{rstu}, \tag{17}
\end{aligned}$$

and

$$\begin{aligned}
\frac{1}{g^{1/2}} \frac{\delta}{\delta g_{mn}} W_{10} &= 3R_{pqr}{}^{m;p} R_s{}^{rqn;s} + 3R_{pqr}{}^n R^{pmrs;q} + 3R_{pqr;s}{}^p R^{qmrs;n} \\
&\quad + 3R_{pqr;s}{}^p R^{qmrs;n} - \frac{3}{2} R_p^m{}_{;q} R_{rs}{}^n R^{psqr} - \frac{3}{2} R_p^n{}_{;q} R_{rs}{}^m R^{psqr} \\
&\quad + \frac{3}{2} R_p^n{}_{;qr}{}^r R^{psqm} + \frac{3}{2} R_p^m{}_{;qr}{}^r R^{psqn} - 3R_{pqr}{}^m R_s{}^q{}^n R^{psrt} \\
&\quad + \frac{3}{2} R_{pqr}{}^n{}^q R^{pmrs} - \frac{3}{2} R_{pqr;s}{}^{sq} R^{pmrn} + \frac{3}{2} R_{pqr}{}^m{}^q R^{pnrs} \\
&\quad - \frac{3}{2} R_{pqr;s}{}^{sq} R^{pmrn} + \frac{1}{2} R_{pqr;s} R_{tu}{}^{p r} R^{qtsu}. \tag{18}
\end{aligned}$$

As there are numerous identities involving the Riemann tensor, its covariant derivatives and contractions, the form of  $\langle T_b^a \rangle_{ren}$  is, of course, not unique and depends on adopted simplification strategies. Here we presented our results in the form that we have found useful in the further calculations. It should be noted that the resulting renormalized stress-tensor of the massive scalar field depends on the coupling constant in a complicated way, and in a general spacetime it divides naturally into four terms

$$\langle T_a^b \rangle_{ren} = \frac{1}{30} \left( \xi - \frac{1}{6} \right) T^{(1)b}_a + \frac{1}{2} \left( \xi - \frac{1}{6} \right)^2 T^{(2)b}_a + \left( \xi - \frac{1}{6} \right)^3 T^{(3)b}_a + T^{(4)b}_a, \quad (19)$$

where

$$T^{(1)ab} = \frac{1}{96\pi^2 m^2} g^{-1/2} \frac{\delta}{\delta g_{ab}} (W_5 - W_4), \quad (20)$$

$$T^{(2)ab} = \frac{1}{96\pi^2 m^2} g^{-1/2} \frac{\delta}{\delta g_{ab}} W_1, \quad (21)$$

$$T^{(3)ab} = \frac{1}{96\pi^2 m^2} g^{-1/2} \frac{\delta}{\delta g_{ab}} W_3, \quad (22)$$

$$T^{(4)ab} = \frac{1}{96\pi^2 m^2} g^{-1/2} \left( \beta \frac{\delta}{\delta g_{ab}} W_1 + \alpha_2 \frac{\delta}{\delta g_{ab}} W_2 + \sum_{i=6}^{10} \alpha_i \frac{\delta}{\delta g_{ab}} W_i \right), \quad (23)$$

and

$$\beta = \frac{1}{252} - \frac{\xi}{30}. \quad (24)$$

Inspection of eqs. (9-18) shows that variational derivatives of  $W_1$  and  $W_3$ , with respect to the metric tensor vanish in  $R = 0$  geometries, and, additionally, that of  $W_2$ ,  $W_4$ ,  $W_6$ , and  $W_7$  vanish for the Ricci-flat geometries. Moreover, one has important simplifications of the general stress-energy tensor for the conformally coupled massive fields as there is no need to compute  $T^{(1)ab}$ ,  $T^{(2)ab}$ , and  $T^{(3)ab}$ . Finally we observe that the analogous expression of the stress-energy tensor of the quantized massive spinor and vector fields differs only by the numerical coefficients  $\alpha_i$ . Inserting appropriate coefficients listed in the Table I into (7), one may easily generalize our discussion to the fields of higher spins. Note however, that to obtain the appropriate result for the neutral spinor field one has to multiply the renormalized effective action by the factor 1/2.

### III. ELECTRICALLY CHARGED NONLINEAR BLACK HOLE

As is well known the Reissner-Nordström line element is the only static and asymptotically flat solution of the Einstein- Maxwell equations representing a black hole of mass  $M$  and electric charge  $e$ . The appropriate line element has the form

$$ds^2 = -U(r)dt^2 + V^{-1}(r)dr^2 + r^2(\sin^2\theta d\phi^2 + d\theta^2), \quad (25)$$

where the metric functions  $U(r)$  and  $V(r)$  are given by

$$U(r) = V(r) = 1 - \frac{2M}{r} + \frac{e^2}{r^2}. \quad (26)$$

Because of its simplicity the RN solution may be studied analytically; for  $e^2 < M^2$  the equation  $g_{00} = 0$  has two positive roots

$$r_{\pm} = M \pm (M^2 - e^2)^{1/2}, \quad (27)$$

and the larger root represents the location of the event horizon, while  $r_-$  is the inner horizon. In the limit  $e^2 = M^2$  horizons merge at  $r = M$ , and the RN solution degenerates to the extremal one. The singularity of the RN line element that one encounters at  $r = 0$  is a non-removable curvature singularity, while those at  $r_{\pm}$  are merely spurious singularities that may be easily removed by a suitable choice of coordinates.

Recent interest in the nonlinear electrodynamics is partially motivated, beside a natural curiosity, by the fact that the theories of this type frequently arise in modern theoretical physics. For example they appear as effective theories of string/M-theory. Moreover, one expects that it should be possible to construct solutions to the coupled system of the Einstein field and equations of the nonlinear electrodynamics, which may be interpreted as representing globally regular black hole geometries, avoiding thus the singularity problem. As the nonlinear electrodynamics in the weak field limit coincides with the Maxwell theory, one expects that the appropriate solution should approach at large distances the RN solution.

An interesting solution of this type, representing spacetime of the regular black hole with mass  $M$  and charge  $e$  has been constructed recently by Ayón-Beato and García [17]. The appropriate line element is given by (25) with

$$U(r) = V(r) = 1 - \frac{2M}{r} \left[ 1 - \tanh\left(\frac{e^2}{2Mr}\right) \right]. \quad (28)$$

For  $e = 0$  the ABG solution reduces to the Schwarzschild solution; for small values of the charge it differs from the Reissner-Nordström solution by terms of order  $O(e^6)$ . At large distances the metric structure of (28) also closely resembles that of the RN solution. Indeed, expanding  $U(r)$  in a power series one concludes that the ABG solution behaves asymptotically as

$$U(r) = V(r) = 1 - \frac{2M}{r} + \frac{e^2}{r^2} - \frac{e^6}{12M^2r^4} + O\left(\frac{1}{r^6}\right). \quad (29)$$

Instead of referring to numerical calculations at this stage of analyses of the ABG geometry, we show that although the metric coefficient  $U(r)$  is a complicated function of  $r$ , the location of the horizons may be elegantly expressed in terms of the Lambert functions [18]. Indeed, making use of the substitution  $r = Mx$  and  $e^2 = q^2M^2$ , and subsequently introducing a new unknown function  $W$  by means of the relation

$$x = -\frac{4q^2}{4W - q^2}, \quad (30)$$



one arrives at

$$\exp(W)W = -\frac{q^2}{4} \exp(q^2/4). \quad (31)$$

Since the Lambert function is defined as

$$\exp(W(s))W(s) = s, \quad (32)$$

one concludes that the location of the horizons as a function of  $q = |e|/M$ , is given by the real branches of the Lambert functions

$$x_+ = -\frac{4q^2}{4W(0, -\frac{q^2}{4} \exp(q^2/4)) - q^2}, \quad (33)$$

and

$$x_- = -\frac{4q^2}{4W(-1, -\frac{q^2}{4} \exp(q^2/4)) - q^2}. \quad (34)$$

The functions  $W(0, s)$  and  $W(-1, s)$  are the only real branches of the Lambert function with the branch point at  $s = -1/e$ , where  $e$  is the base of natural logarithms. The horizons  $r_+$  and  $r_-$  for

$$|e|/M = 2W^{1/2}(1/e), \quad (35)$$

merge at

$$x_{extr} = \frac{4W(1/e)}{1 + W(1/e)}, \quad (36)$$

where  $W(s)$  is a principal branch of the Lambert function  $W(0, s)$ . Numerically one has

$$x_{extr} = 0.871, \quad (37)$$

and

$$\frac{|e|}{M} = 1.056. \quad (38)$$

Inspection of (33) and (34) shows an interesting feature of the ABG geometry: the black hole solution exists for  $q$  greater than the analogous ratio of the parameters of the RN solution.

The location of  $r_+$  and  $r_-$  as a function of  $q$  for the charged black holes of both types are displayed in Fig. 1; its numerical values for some characteristic values of  $|e|/M$  are presented in Table II. Inspection of the figure shows that locations of the event horizons of the RN and ABG solutions are almost indistinguishable for, approximately,  $|e|/M \lesssim 0.7$ , whereas the differences between the inner horizons are more prominent. The latter differences are irrelevant here as in our analyses we shall confine ourselves to the static region exterior to the event horizon. Generally, for a given  $q$ ,  $r_+$  of the RN black hole is always greater than  $r_+$  of the ABG geometry.

We remark here that the global structure of the ABG spacetime is similar to that of RN, with one notable distinction. Simple analysis shows that the curvature invariants of the curvature tensor,  $R$ ,  $Ricci^2$ , and  $Riem^2$  are regular as  $r \rightarrow 0$ , and, moreover, other differential invariants of the Riemann tensor and its covariant derivatives also exhibit regularity there. One concludes therefore that the ABG geometry for  $q \leq q_{extr}$  represents the regular black hole solution. While this property of the ABG solution is not surprising it should be remembered that earlier efforts have been in unsuccessful in this regard.

By means of the Wick rotation one obtains the Euclidean version of (25) with (28), which has no conical singularity provided the time coordinate is periodic with the period given by

$$\beta_H = 4\pi \lim_{r \rightarrow r_+} [U(r)V^{-1}(r)]^{1/2} \left( \frac{dU}{dr} \right)^{-1}. \quad (39)$$

Making use of elementary properties of the hyperbolic functions one has

$$\beta_H = 4\pi \left[ \frac{1}{r_+} - \frac{e^2}{r_+^2 M} \left( 1 - \frac{r_+}{4M} \right) \right]^{-1}. \quad (40)$$

We recall also that analogous period of the Euclideanized RN geometry is given by

$$\beta_H = 4\pi \left( \frac{2M}{r_+^2} - \frac{2e^2}{r_+^3} \right)^{-1}. \quad (41)$$

In the limit  $e \rightarrow 0$  both (40) and (41) tend to the Schwarzschild value  $8\pi M$  whereas in the extremality limit  $\beta_H$  tends to infinity. As the Hawking temperature is proportional to the inverse of the period  $\beta_H$  one concludes that in the extremality limit the Hawking temperature of the ABG black hole vanishes. Moreover, closer analysis indicates that for a given  $e$  and  $M$  the ABG black hole is hotter than its RN counterpart characterized by the same values of the parameters. Of course, as expected, for small electric charges both temperatures are practically indistinguishable.

#### IV. RENORMALIZED STRESS-ENERGY TENSOR IN THE SPACETIME OF ELECTRICALLY CHARGED BLACK HOLE

In this chapter the method described in Sec. II is used to construct the renormalized stress-energy tensor of the quantized massive scalar fields in the ABG and extremal ABG spacetimes in the region exterior to the event horizon. As there are important simplifications for  $\xi = 1/6$  we shall consider only the conformal coupling.

The analogous tensor in the RN geometry has been evaluated in Ref.[8] by means of the sixth-order WKB approximation of the solution to the scalar field equation and the summation thus obtained mode functions by means of the Abel-Plana formula. This result has been rederived and extended to the case of other spins, using simplified version of Eqs. (19-24) valid in the spacetimes with vanishing curvature scalar [16].

Calculating the components of the Riemann tensor, its contractions and required covariant derivatives, inserting the results into (9-18), performing appropriate simplifications, and

finally constructing the renormalized stress-energy tensor, after rather lengthy calculations one has

$$\begin{aligned}
\frac{1}{\gamma\alpha}\langle T_t^t \rangle_{ren} = & - \left\{ 576 \gamma M^7 r^6 (-626 \gamma M + 285 r) \right. \\
& - 576 \delta e^2 M^5 r^5 (170 \gamma^2 M^2 - 669 \gamma M r + 270 r^2) \\
& + 48 \delta e^4 M^4 r^4 [186 (-47 + 181 \beta) \gamma^2 M^2 \\
& + (3967 - 38132 \beta + 34165 \beta^2) M r + 8520 \beta r^2] \\
& + 12 \delta e^8 M^2 r^2 [2 \gamma^2 M^2 (3431 \beta^2 + 47307 \beta^3 - 2976 - 32264 \beta) \\
& + M r (2824 + 52712 \beta - 58927 \beta^2 - 79068 \beta^3 + 82459 \beta^4) \\
& + 5904 \beta (-2 + 3 \beta^2) r^2] \\
& - 96 \delta e^6 M^3 r^3 [6 (-1297 - 283 \beta + 3576 \beta^2) \gamma^2 M^2 \\
& + (6730 - 5993 \beta - 20190 \beta^2 + 19453 \beta^3) M r \\
& - 1455 r^2 (1 - 3 \beta^2)] \\
& - 12 \delta e^{10} M r [2 \gamma^2 M^2 (1302 - 2253 \beta - 12187 \beta^2 \\
& + 2485 \beta^3 + 12449 \beta^4) - M r (2524 - 4653 \beta \\
& - 18930 \beta^2 + 23420 \beta^3 + 18930 \beta^4 - 21291 \beta^5) \\
& + 298 (2 - 15 \beta^2 + 15 \beta^4) r^2] \\
& + \delta e^{12} [2 \gamma^2 M^2 (693 + 4629 \beta - 5370 \beta^2 - 19490 \beta^3 \\
& + 4745 \beta^4 + 15409 \beta^5) - 3 M r (231 + 2720 \beta - 4645 \beta^2 \\
& - 9600 \beta^3 + 12785 \beta^4 + 7200 \beta^5 - 8691 \beta^6) \\
& \left. + 120 \beta r^2 (17 - 60 \beta^2 + 45 \beta^4) \right\}, \tag{42}
\end{aligned}$$

$$\begin{aligned}
\frac{1}{\gamma M \alpha} \langle T_r^r \rangle_{ren} = & 4032 \gamma M^6 (22 \gamma M - 15 r) r^6 \\
& + \delta^2 e^{12} \gamma [(270 - 558 \beta - 1500 \beta^2 + 2060 \beta^3 + 1350 \beta^4 - 1622 \beta^5) M \\
& - 15 (9 - 50 \beta^2 + 45 \beta^4) r] \\
& + 12 \delta e^2 r \{ -48 M^4 r^4 (478 \gamma^2 M^2 - 391 \gamma M r + 54 r^2) \\
& + 4 e^2 M^3 r^3 [6 (101 + 873 \beta) \gamma^2 M^2 \\
& - (707 + 3148 \beta - 3855 \beta^2) M r + 472 \beta r^2] \\
& + e^6 M r [2 (-544 - 1304 \beta + 957 \beta^2 + 2041 \beta^3) \gamma^2 M^2 \\
& + r (392 + 408 \beta - 1717 \beta^2 - 612 \beta^3 + 1529 \beta^4) M + 40 \beta r (2 - 3 \beta^2)] \\
& - 8 e^4 M^2 r^2 [6 (-73 + 35 \beta + 222 \beta^2) \gamma^2 M^2 \\
& + r (170 - 387 \beta - 510 \beta^2 + 727 \beta^3) M + 11 (3 \beta^2 - 1) r^2] \\
& + e^8 [2 (18 + 407 \beta + 441 \beta^2 - 487 \beta^3 - 551 \beta^4) \gamma^2 M^2
\end{aligned}$$

$$\begin{aligned}
& +r(4 - 287\beta - 30\beta^2 + 676\beta^3 + 30\beta^4 - 393\beta^5)M \\
& +2(2 - 15\beta^2 + 15\beta^4)r^2\}, \tag{43}
\end{aligned}$$

and

$$\begin{aligned}
\frac{1}{\gamma\alpha}\langle T_\theta^\theta \rangle_{ren} &= 576\gamma M^7(734\gamma M - 315r)r^6 \\
& +\delta e^2\{-576M^5r^5(2202\gamma^2M^2 - 1313\gamma Mr + 162r^2) \\
& +48e^2M^4r^4[6(1399 + 3777\beta)\gamma^2M^2 + r(-3353 - 10914\beta + 14267\beta^2)M \\
& +1976\beta r^2] - 12e^6M^2r^2[2(-202 - 1198\beta + 749\beta^2 + 2161\beta^3)\gamma^2M^2 \\
& +r(154 + 1184\beta - 2227\beta^2 - 1776\beta^3 + 2665\beta^4)M + 92\beta(-2 + 3\beta^2)r^2] \\
& -48e^4M^3r^3[6(-91 + 649\beta + 1042\beta^2)\gamma^2M^2 \\
& +r(873 - 2308\beta - 2619\beta^2 + 4054\beta^3)M + 206(-1 + 3\beta^2)r^2] \\
& +12e^8Mr[2(80 - 519\beta - 1169\beta^2 + 1089\beta^3 + 1755\beta^4)\gamma^2M^2 \\
& +r(-176 + 639\beta + 1320\beta^2 - 2716\beta^3 - 1320\beta^4 + 2253\beta^5)M \\
& +20(2 - 15\beta^2 + 15\beta^4)r^2] \\
& -e^{10}[2(129 + 441\beta - 1590\beta^2 - 2750\beta^3 + 2105\beta^4 + 3001\beta^5)\gamma^2M^2 \\
& +3r(-43 - 272\beta + 781\beta^2 + 960\beta^3 - 2005\beta^4 - 720\beta^5 + 1299\beta^6)M \\
& +4\beta(17 - 60\beta^2 + 45\beta^4)r^2]\}, \tag{44}
\end{aligned}$$

where

$$\alpha^{-1} = 96\pi^2 m^2 \times 60480M^5r^{15}, \tag{45}$$

$$\beta = \tanh \frac{e^2}{2Mr}, \tag{46}$$

$$\gamma = 1 - \beta, \tag{47}$$

and

$$\delta = 1 + \beta. \tag{48}$$

Obtained tensor is, as expected, covariantly conserved, and as could be easily verified in the limit  $e = 0$ , it reduces to the stress-energy tensor constructed in the Schwarzschild spacetime by Frolov and Zel'nikov.

Equations (8-18) may be employed also in the RN geometry. Since the scalar curvature is zero there, both  $T^{(2)ab}$  and  $T^{(3)ab}$  vanishes, and the resulting tensor exhibits simple linear dependence on the coupling constant. Indeed, repeating the calculations for the line element (26), one has [8,16]

$$\langle T_a^b \rangle_{ren}^{(0)} = C_a^b + \left( \xi - \frac{1}{6} \right) D_a^b, \quad (49)$$

where

$$C_t^t = -\frac{1}{30240 \pi^2 m^2 r^{12}} \left( 1248 e^6 - 810 r^4 e^2 + 855 M^2 r^4 + 202 r^2 e^4 - 1878 M^3 r^3 + 1152 M r^3 e^2 + 2307 M^2 r^2 e^2 - 3084 r M e^4 \right), \quad (50)$$

$$C_r^r = \frac{1}{30240 \pi^2 m^2 r^{12}} \left( 444 e^6 - 1488 M r^3 e^2 + 162 r^4 e^2 + 842 r^2 e^4 - 1932 r M e^4 + 315 M^2 r^4 + 2127 M^2 r^2 e^2 - 462 M^3 r^3 \right), \quad (51)$$

and

$$C_\theta^\theta = -\frac{1}{30240 \pi^2 m^2 r^{12}} \left( 3044 r^2 e^4 - 2202 M^3 r^3 - 10356 r M e^4 + 3066 e^6 - 4884 r^3 M e^2 + 9909 r^2 M^2 e^2 + 945 M^2 r^4 + 486 r^4 e^2 \right). \quad (52)$$

Since we are interested in the conformally coupled massive scalar fields, the exact form of the  $D_a^b$  tensor is irrelevant.

Now, we shall address the question of how the differences between the geometry of the black hole spacetimes constructed within the framework of the Einstein-Maxwell theory on the one hand and the nonlinear electrodynamics coupled to the General Relativity on the other, are reflected in the overall behavior of the components of the stress-energy tensors. To answer this, let us analyze numerically  $\langle T_a^b \rangle_{ren}$  in both cases. The results of our calculations are presented graphically in Figs. 2 - 10. The plots of the time, radial, and angular components of the stress-energy tensor of the quantized massive scalar field as a functions of the (rescaled) radial coordinate in the spacetimes of ABG and RN black holes for three exemplar values of the ratio  $|e|/M = 0.1, 0.5$  and  $0.95$ , are supplemented by similar plots drawn for the extremal black holes. Inspection of the figures indicates that there are striking qualitative similarities between the RN and ABG solutions for a given  $q$ . Moreover, for small values of the ratio the curves are practically undistinguishable from each other, and, as expected, noteworthy differences occur only for the black holes at and near the extremality limit. Since at large distances the line element (28) approaches that of the RN, the most interesting region is the neighborhood of the black hole event horizon. From Eq.(19) we know that the renormalized stress-energy tensor depends on the coupling constant  $\xi$  in a complicated way, and, therefore, one should not expect that such similarities occur also in a general case.

Specifically, the dependence of  $\langle T_t^t \rangle_{ren}$  constructed in the spacetime of the nonlinear black hole and the RN geometry on  $r/r_+$  for  $|e|/M = 0.1, 0.5, 0.95$ , are shown in Figs. 2 and 3, respectively. In Fig. 4 similar curves are drawn for the extremal black holes. In the most interesting region, i.e., in the vicinity of the event horizon, the energy density,  $\rho = -\langle T_t^t \rangle_{ren}$ , is negative and decreases with increasing of  $|e|/M$ .

As is seen in Figs. 5 -7, the radial component of the stress-energy tensor is everywhere positive, and the horizon values of the radial pressure,  $p_r = \langle T_r^r \rangle_{ren}$ , increases with increasing  $|e|/M$ .

Of all components of the renormalized stress-energy tensor, the most complicated behavior exhibits the angular pressure  $p_\theta = \langle T_\theta^\theta \rangle_{ren}$  (Figs 8 - 10). Indeed, for the ABG black hole the angular pressure is positive on the event horizon for  $|e|/M \lesssim 0.937$  and negative for larger values of the ratio. Moreover, for  $q \lesssim 0.903$ ,  $\langle T_\theta^\theta \rangle_{ren}$  has a maximum at  $r = r_+$ , whereas for larger values the angular pressure has its maximum away from the event horizon. Similarly, for the RN black hole  $p_\theta$  is positive for  $q \lesssim 0.927$  and it has its maximum away from the event horizon for  $q \gtrsim 0.864$ .

It could be checked by a direct calculation that

$$\lim_{r \rightarrow r_+} \left( \langle T_t^t \rangle_{ren} - \langle T_r^r \rangle_{ren} \right) \left\{ 1 - \frac{2M}{r} \left[ 1 - \tanh \frac{e^2}{2Mr} \right] \right\}^{-1} \quad (53)$$

remains finite at the event horizon. We observe that since the DeWitt-Schwinger approximation is local and the geometry at the event horizon is regular, one expects that the renormalized stress-energy tensor is also regular there.

It should be stressed once again that for arbitrary curvature coupling one has to incorporate also the terms  $T^{(1)ab}$ ,  $T^{(2)ab}$ , and  $T^{(3)ab}$ , that may considerably modify the results. Moreover, inspection of the Table I shows that for the neutral massive spinor and vector fields in the ABG spacetime one has to use the full system (9 - 18) while in the geometry of the RN black hole, the terms (9) and (11) do not contribute to the final result.

## V. CONCLUDING REMARKS

In this paper we have constructed the renormalized stress-energy tensor of the massive conformally coupled scalar fields in the spacetime of the electrically charged black hole, being the solution of the coupled Einstein equation and the equation of nonlinear electrodynamics. A regular solution of this type has been recently given by Ayón-Beato and García. The method employed here is based on the observation that the first order effective action could be expressed in terms of the traced coincidence limit of the coefficient  $a_3$ . The general  $\langle T_a^b \rangle_{ren}$ , which has been obtained by functional differentiation of the effective action with respect to a metric tensor, has been applied in the spacetime of the nonlinear black hole. Since the Reissner-Nordström line element and ABG solution are practically indistinguishable from each other for small values of  $|e|/M$ , one expects that this similarity should be reflected in the behavior of the renormalized stress-energy tensor. Explicit calculations confirm this hypothesis and show that important differences between appropriate tensors,  $\langle T_a^b \rangle_{ren}$ , evaluated in the spacetime of the RN black hole and that of ABG occur, as expected, near the extremality limit. For small  $q$  constructed tensors are practically indistinguishable. Moreover, analyses of the Hawking temperatures indicate that for a given mass and electric charge, the ABG black hole is hotter than its RN black hole counterpart. Since notable differences appear for temperatures close to zero one can ascribe this to the different ways of approaching the extremality limits.

Apart from obvious extensions of our results to the massive scalar fields with arbitrary curvature coupling and to fields of higher spins, let us mention an interesting and important direction for future work. It is a problem of the back reaction of the quantized fields upon spacetime geometry of the ABG black hole, which may be studied perturbatively by means

of the semiclassical Einstein field equations with a source term given by the renormalized stress-energy tensor of the quantized massive field and the classical stress-energy tensor of the background nonlinear electromagnetic field. To guarantee the renormalizability at that level, the semiclassical equations should contain higher derivative geometric terms. It is especially important in view of the recent claim that the semiclassical zero temperature RN black holes do not exist [14].

It should be stressed that the DeWitt-Schwinger expansion is local, and, therefore, does not describe particle creation which is a nonperturbative and nonlocal phenomenon. The method also breaks down in strong or rapidly varying gravitational fields, and, moreover, the massless limit leads to the nonphysical divergences. However, it is expected that for sufficiently massive scalar field the DeWitt-Schwinger approximation provides a good approximation of the exact renormalized stress-energy tensor.

- 
- [1] B. S. DeWitt, Phys. Reports **19 C**, 297 (1975).
  - [2] J. S. Schwinger, Phys. Rev. **82**, 664 (1951).
  - [3] V. P. Frolov and A. I. Zel'nikov, Phys. Lett. B **115**, 372 (1982).
  - [4] V. P. Frolov and A. I. Zel'nikov, Phys. Lett. B **123**, 197 (1983).
  - [5] V. P. Frolov and A. I. Zel'nikov, Phys. Rev. D **29**, 1057 (1984).
  - [6] V. P. Frolov, Proceedings of the Lebedev Institute of the Academy of Science of USSR **169** (1986).
  - [7] V. P. Frolov and I. D. Novikov, *Black Hole Physics* (Kluwer Dordrecht 1998).
  - [8] P. R. Anderson, W. A. Hiscock, and D. A. Samuel, Phys. Rev. D **51**, 4337 (1995).
  - [9] W. A. Hiscock, S. L. Larson, and P. R. Anderson, Phys. Rev. D **56**, 3571 (1997).
  - [10] B. E. Taylor, W. A. Hiscock, and P. R. Anderson, Phys. Rev. D **55**, 6116 (1997).
  - [11] S. V. Sushkov, Phys. Rev. D **62**, 064007 (2000).
  - [12] S. V. Sushkov, gr-qc/0009028.
  - [13] B. E. Taylor, W. A. Hiscock, and P. R. Anderson, Phys. Rev. D **61**, 084021 (2000).
  - [14] P. R. Anderson, W. A. Hiscock, and B. E. Taylor, Phys. Rev. Lett. **85**, 2438 (2000).
  - [15] H. Koyama, Y. Nambu, and A. Tomimatsu, Mod. Phys. Lett. A **15**, 815 (2000).
  - [16] J. Matyjasek, Phys. Rev. D **61**, 124019 (2000).
  - [17] E. Ayón-Beato and A. García, Phys. Lett. B **464**, 25 (1999).
  - [18] R. M. Corless, G. H. Gonnet, D.E.G. Hare, D. J. Jeffrey, and D. E. Knuth, Adv. Comput. Math. **5**, 329 (1996).
  - [19] P. B. Gilkey, J. Diff. Geom, **10**, 601 (1975).
  - [20] P. B. Gilkey, Trans. Am. Math. Soc. **225**, 341 (1977).
  - [21] I. G. Avramidi, hep-th/9510140.
  - [22] I. G. Avramidi, Teor. Mat. Fiz, **79**, 219 (1989).
  - [23] I. G. Avramidi, Nucl. Phys. **B 355**, 712 (1991).
  - [24] I. G. Avramidi, Phys. Lett. B **238**, 92 (1990).

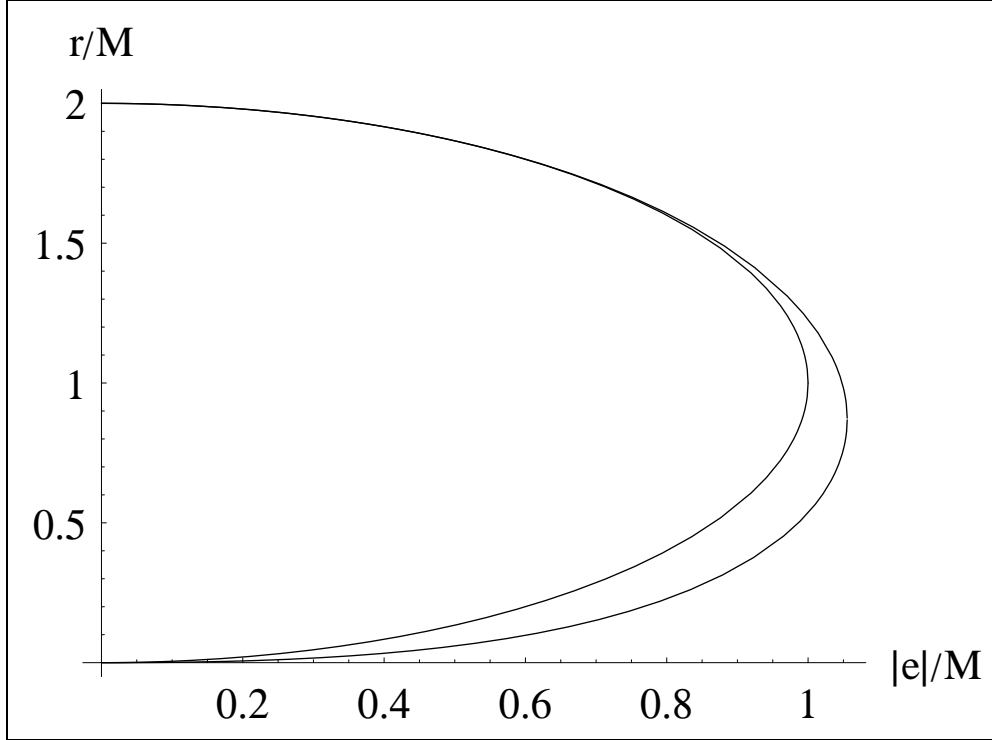


FIG. 1. The location of  $r_+$  (upper branches) and  $r_-$  (lower branches) of the RN and ABG geometries as a function of  $e/M$ . The curve representing horizons of the ABG black hole is shifted to the right with respect to the one which has been determined in the RN spacetime.



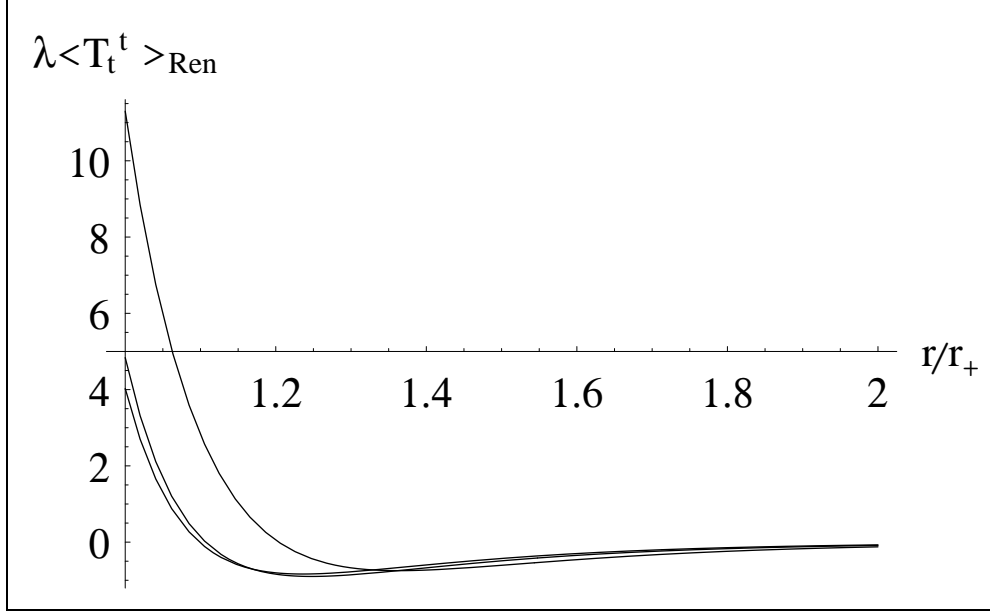


FIG. 2. This graph shows the radial dependence of the rescaled component  $\langle T_t^t \rangle_{ren}$  [ $\lambda = 90(8M)^4 m^2 \pi^2$ ] of the renormalized stress-energy tensor of the massive conformally coupled scalar field in the ABG geometry. From top to bottom the curves are for  $|e|/M = 0.95, 0.5,$  and  $0.1$ . In each case  $\langle T_t^t \rangle_{ren}$  has its positive maximum at  $r = r_+$  and attains negative minimum away from the event horizon.

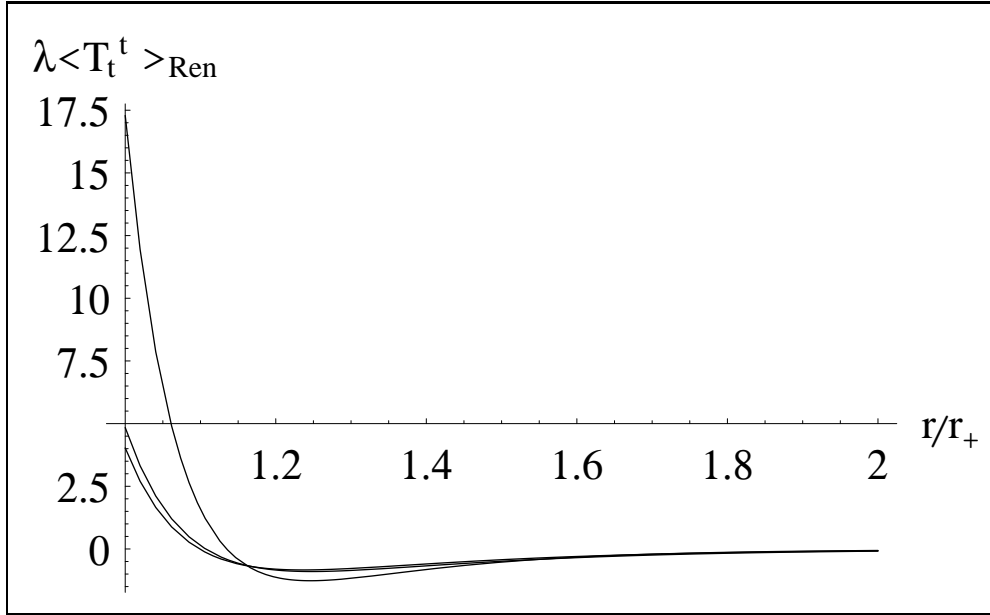


FIG. 3. This graph shows the radial dependence of the rescaled component  $\langle T_t^t \rangle_{ren}$  [ $\lambda = 90(8M)^4 m^2 \pi^2$ ] of the renormalized stress-energy tensor of the massive conformally coupled scalar field in the RN spacetime. From top to bottom the curves are for  $|e|/M = 0.95, 0.5,$  and  $0.1$ . In each case  $\langle T_t^t \rangle_{ren}$  has its positive maximum at  $r = r_+$  and attains negative minimum away from the event horizon.

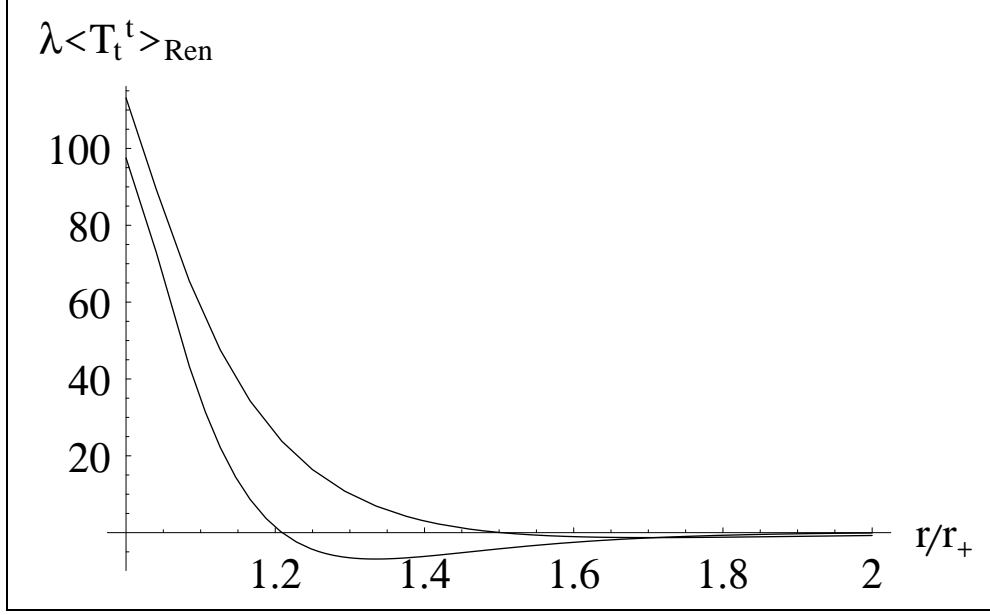


FIG. 4. This graph shows the radial dependence of the rescaled component  $\langle T_t^t \rangle_{ren}$  [ $\lambda = 90(8M)^4 m^2 \pi^2$ ] of the renormalized stress-energy tensor of the massive conformally coupled scalar field. Top to bottom the curves are respectively for the extremal ABG geometry and the extremal RN black hole

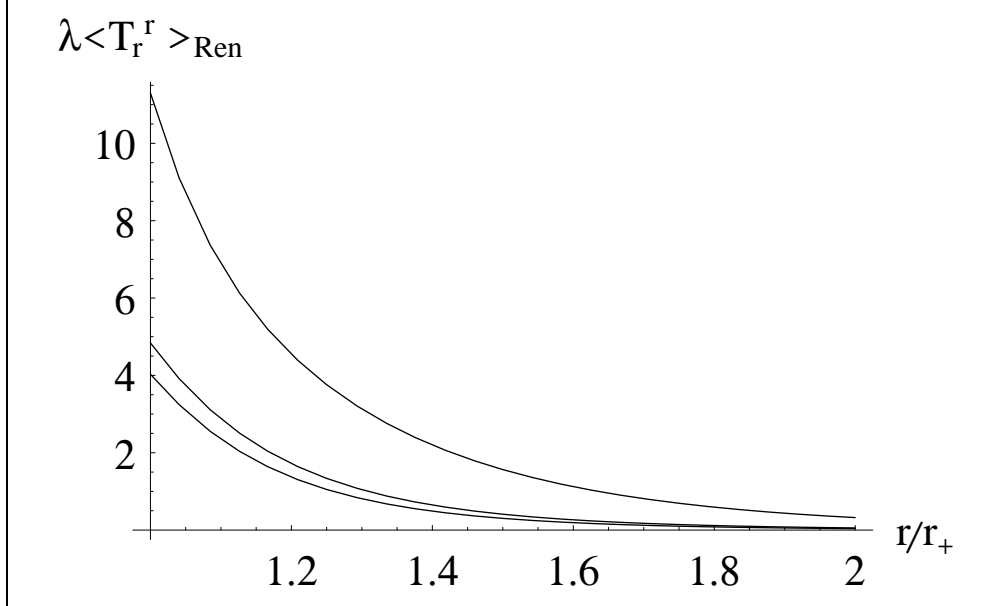


FIG. 5. This graph shows the radial dependence of the rescaled component  $\langle T_r^r \rangle_{ren}$  [ $\lambda = 90(8M)^4 m^2 \pi^2$ ] of the renormalized stress-energy tensor of the massive conformally coupled scalar field in the Ayón-Beato and Gracia geometry. From top to bottom the curves are for  $|e|/M = 0.95, 0.5,$  and  $0.1$ . In each case  $\langle T_r^r \rangle_{ren}$  has its positive maximum at  $r = r_+$  and decreases monotonically with  $r$ .

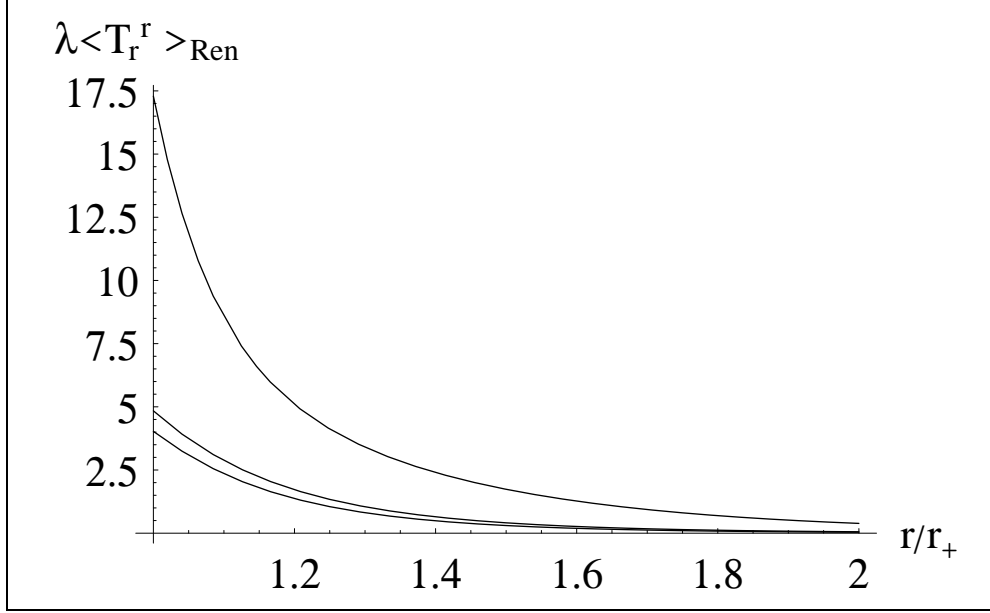


FIG. 6. This graph shows the radial dependence of the rescaled component  $\langle T_r^r \rangle_{ren}$  [ $\lambda = 90(8M)^4 m^2 \pi^2$ ] of the renormalized stress-energy tensor of the massive conformally coupled scalar field in the RN spacetime. From top to bottom the curves are for  $|e|/M = 0.95, 0.5,$  and  $0.1$ . In each case  $\langle T_t^t \rangle_{ren}$  has its positive maximum at  $r = r_+$  and decreases monotonically with  $r$ .

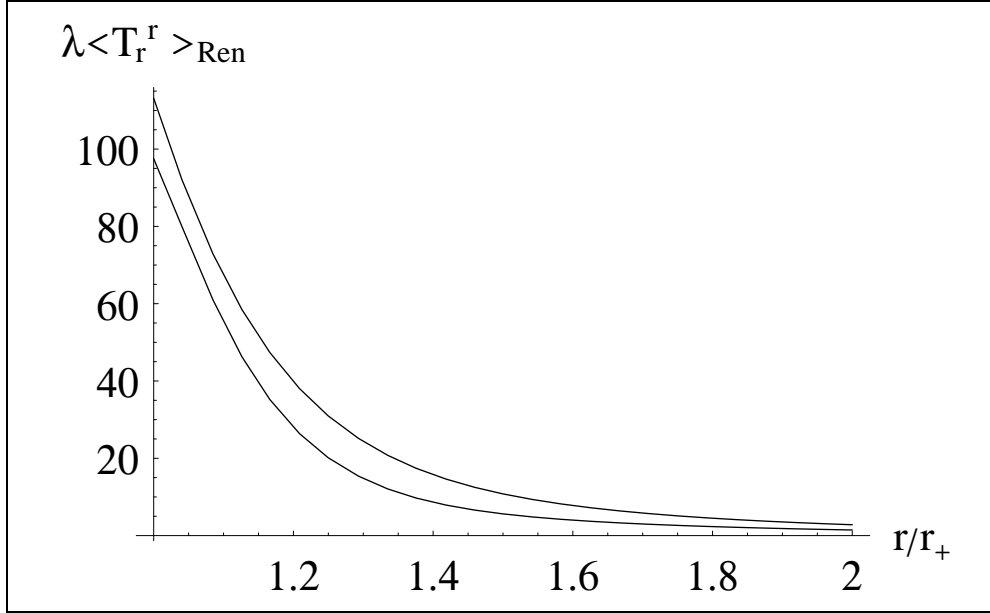


FIG. 7. This graph shows the radial dependence of the rescaled component  $\langle T_r^r \rangle_{ren}$  [ $\lambda = 90(8M)^4 m^2 \pi^2$ ] of the renormalized stress-energy tensor of the massive conformally coupled scalar field. Top to bottom the curves are respectively for the extremal ABG geometry and the extremal RN black hole

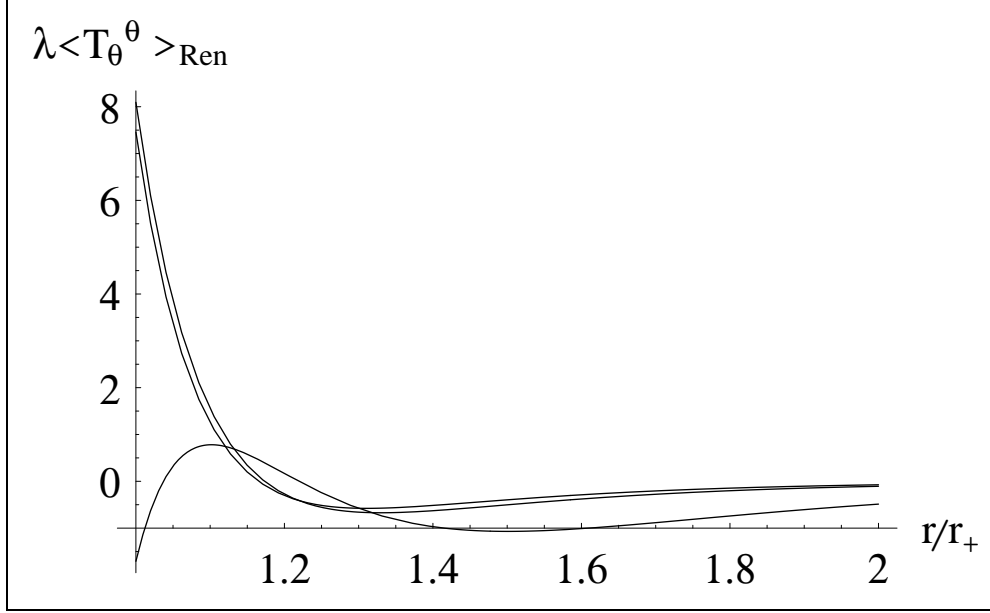


FIG. 8. This graph shows the radial dependence of the rescaled component  $\langle T_\theta^\theta \rangle_{ren}$  [ $\lambda = 90(8M)^4 m^2 \pi^2$ ] of the renormalized stress-energy tensor of the massive conformally coupled scalar field in the ABG geometry. From top to bottom the curves are for  $|e|/M = 0.1, 0.5,$  and  $0.95$ . For  $|e|/M \leq 0.903$ ,  $\langle T_\theta^\theta \rangle_{ren}$  has its positive maximum at  $r = r_+$ . For larger values of the ratio it approaches its maximum away from the event horizon. For  $|e|/M = 0.937$  the angular pressure vanishes on the event horizon.

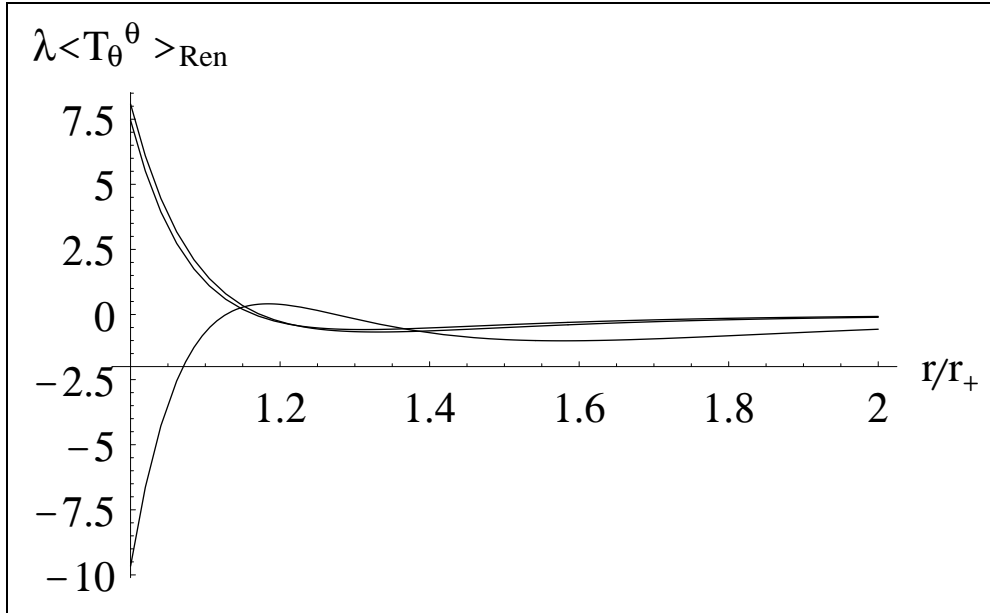


FIG. 9. This graph shows the radial dependence of the rescaled component  $\langle T_\theta^\theta \rangle_{ren}$  [ $\lambda = 90(8M)^4 m^2 \pi^2$ ] of the renormalized stress-energy tensor of the massive conformally coupled scalar field in the RN spacetime. From top to bottom the curves are for  $|e|/M = 0.1, 0.5,$  and  $0.95$ . For  $|e|/M \leq 0.864$ ,  $\langle T_\theta^\theta \rangle_{ren}$  has its positive maximum at  $r = r_+$ . For larger values of the ratio it approaches its maximum away from the event horizon. For  $|e|/M = 0.927$  the angular pressure vanishes at  $r_+$ .

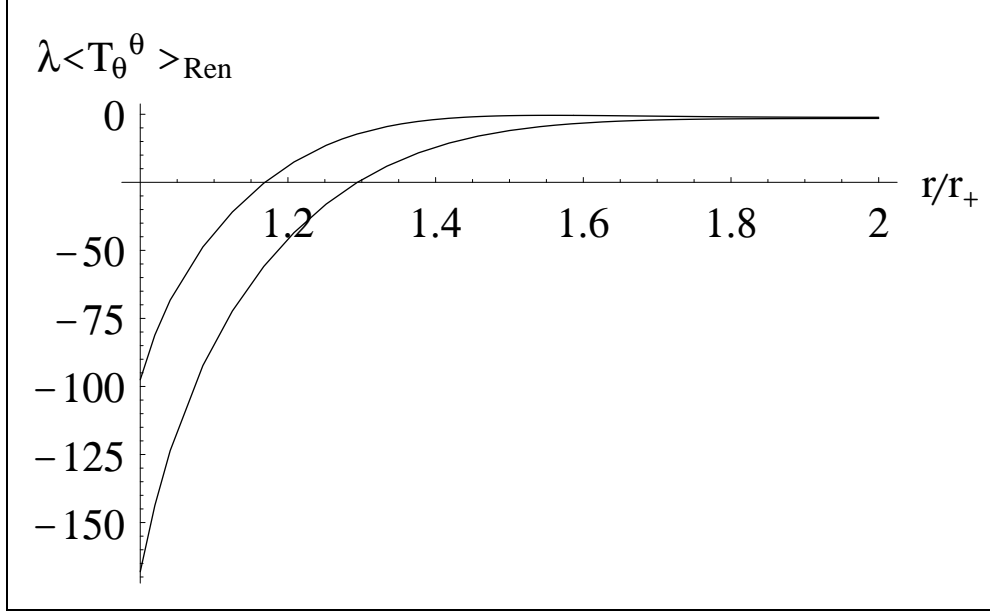


FIG. 10. This graph shows the radial dependence of the rescaled component  $\langle T_\theta^\theta \rangle_{ren}$  [ $\lambda = 90(8M)^4 m^2 \pi^2$ ] of the renormalized stress-energy tensor of the massive conformally coupled scalar field. Top to bottom the curves are respectively for the extremal ABG geometry and the extremal RN black hole.

TABLE I. The coefficients  $\alpha_i^{(s)}$  for the massive scalar, spinor, and vector field

	$s = 0$	$s = 1/2$	$s = 1$
$\alpha_1^{(s)}$	$\frac{1}{2}\xi^2 - \frac{1}{5}\xi + \frac{1}{56}$	$-\frac{3}{140}$	$-\frac{27}{280}$
$\alpha_2^{(s)}$	$\frac{1}{140}$	$\frac{1}{14}$	$\frac{9}{28}$
$\alpha_3^{(s)}$	$\left(\frac{1}{6} - \xi\right)^3$	$\frac{1}{432}$	$-\frac{5}{72}$
$\alpha_4^{(s)}$	$-\frac{1}{30}\left(\frac{1}{6} - \xi\right)$	$-\frac{1}{90}$	$\frac{31}{60}$
$\alpha_5^{(s)}$	$\frac{1}{30}\left(\frac{1}{6} - \xi\right)$	$-\frac{7}{720}$	$-\frac{1}{10}$
$\alpha_6^{(s)}$	$-\frac{8}{945}$	$-\frac{25}{376}$	$-\frac{52}{63}$
$\alpha_7^{(s)}$	$\frac{2}{315}$	$\frac{47}{630}$	$-\frac{19}{105}$
$\alpha_8^{(s)}$	$\frac{1}{1260}$	$\frac{19}{630}$	$\frac{61}{140}$
$\alpha_9^{(s)}$	$\frac{17}{7560}$	$\frac{29}{3780}$	$-\frac{67}{2520}$
$\alpha_{10}^{(s)}$	$-\frac{1}{270}$	$-\frac{1}{54}$	$\frac{1}{18}$

TABLE II. Location of  $r_+$  and  $r_-$  of ABG and RN black holes for exemplar values of  $|e|/M$ .

$ e /M$	$r_-/M$ (ABG)	$r_+/M$ (ABG)	$r_-/M$ (RN)	$r_+/M$ (RN)
0.10	0.001	1.995	0.005	1.995
0.50	0.060	1.866	0.134	1.866
0.95	0.422	1.356	0.688	1.312
extremal	0.871	0.871	1	1